Biosynthesis of Magnesium Oxide Nanoparticles using *Pennisetum Purpureum* and Application in Removal of Cadmium Contaminant from Water

Ebiaguanye, I.T.* and Emeribe, F.O
Department of Chemistry,
Faculty of Physical Sciences,
University of Benin,
Nigeria.

Email: theophilus.ebiaguanye@physci.uniben.com

Abstract

This study evaluated an innovative approach to synthesize magnesium oxide nanoparticles (MgO NPs) through a green synthesis method using Pennisetum purpureum extract as a reducing and stabilizing agent. The green synthesis of MgO NPs is cost-effective and environmentally friendly. Characterization techniques such as X-ray diffraction (XRD), scanning electron microscopy (SEM), and Fourier-transform infrared spectroscopy (FTIR) confirmed the successful synthesis of nanoparticles with unique properties. Debye-Scherrer equation is used for the determination of particle size, which was found to be 15.7nm. The potential application of MgO NPs in the removal of cadmium (Cd) contaminant from water sources was investigated through batch adsorption experiments. Cadmium pollution poses a severe threat to ecosystems and human health due to its toxic nature and persistence in the environment. MgO NPs, with their high surface area and reactivity, efficiently adsorbed and immobilize cadmium ions from water. Adsorption isotherm models indicated that Langmuir isotherm is the best model to describe the adsorption of Cd^{2+} on magnesium oxide nanoparticles prepared by elephant grass extracts. It was found that a removal of greater percent of Cd^{2+} could be accomplished through adsorption with 0.05g of magnesium oxide nanoparticles, an initial concentration of metal at 5ppm pH of 10 and at contact time of 65minutes.

Keywords: *Pennisetum purpureum,* Adsorption, X-ray diffraction, scanning electron microscopy, Fourier-transform infrared spectroscopy.

Introduction

A revolutionary path for scientific progress is the manipulation of materials at the nanoscale (one billion times smaller than a meter). Actually, the term "nanotechnology" encompasses any technology at the nanoscale that has a variety of uses. Developing a basic comprehension of the mechanical, electrical, optical and magnetic properties will be helpful in developing the next generation of functional materials, which have a variety of applications. In recent years, nanotechnology has become a multidisciplinary field. In the fields of medicine, solar energy conversion, catalysis and water treatment. Nanostructures can also provide answers to environmental and technological problems (Nasrollahzadeh *et al.,* 2019). The development of many fields, including biotechnology, medicine, pharmaceuticals, agriculture, food, cosmetics, environment protection, electronics, information technology, construction,

military, energy industry, space industry, and consumer products, among others, was made possible by the invention of nanotechnology (Lee *et al.,* 2020). The creation of nanoparticles with the right size, structure, monodispersity, and morphology is crucial for the aforementioned applications (Khan *et al.,* 2022). Some nanoparticles have an amorphous or crystalline structure with distributed or aggregated single- or multi-crystal solids (Machado *et al.,* 2015). Nanoparticles can be classified into organic nanoparticles, inorganic and Carbon-Based Nanoparticles (Khan *et al.,* 2022).

Nearly all metals can be converted into nanoparticles, including gold, silver, cadmium, cobalt, copper, iron, lead, and zinc, which are often used in the synthesis of nanoparticles (Esa *et al.,* 2020). These nanoparticles exhibit exceptional properties when compared to their metal analogues (Singh *et al.,* 2021). Important metal contaminants like lead and cadmium are frequently of concern when it comes to drinking water, wastewater, and water in general (such as rivers, lakes, and oceans). As a result, they are among the most hazardous metals that are frequently detected in water (Zhou *et al.,* 2020). Exposure to Cd can harm people in a number of ways, including kidney and liver failure, pulmonary edoema, testicular damage, osteomalacia, and harm to the adrenals and hematopoietic system (Tinkov *et al.,* 2018). Through the direct use of nanomaterials for the detection, prevention, and removal of pollutants as well as through the use of superior industrial design techniques and the creation of environmentally friendly goods, nanotechnology has the potential to improve the environment. Hence the need to employ nanotechnology in the removal of Cadmium from these water bodies.

One common chemical used for the synthesis of magnesium oxide nanoparticles (MgOPNS) is sodium hydroxide (NaOH). This serves as both a reactant and a stabilizing agent in the synthesis process. It helps in the hydrolysis of magnesium salts to form magnesium hydroxide, which then undergoes further calcination to produce magnesium oxide nanoparticles (Sathishkumar *et al.,* 2010). This process has potential harmful effects such as Air pollution, corrosive nature, environmental impact e.t.c.

 The use of elephant grass for the biological synthesis of MgONPs has several advantages over chemical methods, including, low toxicity, high efficiency, cost effectiveness, biocompatibility, minimal waste generation and the ability to produce nanoparticles of varying sizes and shapes. In addition, this approach is sustainable and environmentally friendly, as it does not require the use of hazardous chemicals.

This research work is solely focused on the use of magnesium oxide nanoparticles using *Pennisetum purpureum* and it's application in treatment of cadmium contaminant in water where Adsorption, X-ray diffraction, scanning electron microscopy, Fourier-transform infrared spectroscopy are employed to ensure the success of this process.

MATERIALS AND METHODS

Collection and Preparation of Plant Sample
Fresh *Pennisetum purpureum* were obtained from BDPA community Benin City, Edo State. It was identified and authenticated by Dr H. A. Akinnibosun at the herbarium unit of the Department of Plant Biology and Biotechnology, University of Benin, Benin city with voucher specimen number UBH-C102. Fresh leaves of *P. purpureum* were washed with distilled water to remove dirt and dust on the surface of the leaves. The thoroughly washed leaves were air dried for 7 days at room temperature. The dried leaves were pulverized into fine powder,

which was used for further analysis. *P. purpureum* extraction was conducted with reference to the method reported by Fatiqin *et al.*, 2021. 10g of the elephant grass powder was weighed using a weighing balance and was added to 100ml of distilled water. The mixture was boiled at 60^0C for 20minutes. The solution was allowed to cool and filtered using filter paper, and the filtrate was collected for the green synthesis of MgO nanoparticles.

Synthesis of Magnesium Oxide Nanoparticles

The synthesis of MgO NPs was done with reference to the method reported by (Munjah *et al.*, 2017with little modification.

Preparation of Cd²⁺ contaminated water

Salt used: $CdCl_2.H_2O$ (molecular weight =201.32g)
1.79g was weighed from the cadmium salt and diluted in a 1L volumetric flask to prepare a 1000ppm stock solution of cadmium ion (Cd^{2+}) by dividing the molecular weight of Cadmium chloride monohydrate by the atomic weight of the cadmium
Other working solutions were prepared for various adsorption studies from the stock solution (5, 10, 15, 20 and 25) ppm of Cd^{2+} (Singh *et al.,* 2021).

Adsorption Studies and Optimization Studies

The experiment was conducted in batches to establish the adsorption isotherm equilibrium. The removal percentage (R, %) and the equilibrium adsorption capacity of the adsorbent ($q_{e,}\ mg/g$) can be calculated (Saod *et al.,* 2023) :

$$\%R = \frac{C_O - C_e}{C_o} \times 100$$

$$q_e = \frac{C_O - C_e}{m} \times V$$

C_o and Ce (mg/L), represent the initial and equilibrium concentration of metal ions, respectively. V (L) represent the solution volume, m (g) is the adsorbent weight.

Effect of Initial Concentration

Initial concentration was varied at different intervals (5ppm, 10ppm, 15ppm, 20ppm, 25ppm). 100mL was measured from prepared working solutions (5, 10, 15, 20, and 25) ppm into 5 bottles and 0.01g was measured into all 5 bottles. All five bottles were put in the mechanical shaker for 5minutes and centrifuged for 15 mins. All centrifuged samples were taken to the AAS for analysis.

Effect of Adsorbent Dosage

This study was carried out to know what amount of adsorbent (MgO NP) will adsorbed heavy metal more between (0.01- 0.05)g hence, the optimum dosage. 100mL of the prepared 5ppm Cd^{2+} working solution was weighed into 5 bottles, different adsorbent dosage was weighed into the 5 bottles (0.01, 0.02, 0.03, 0.04, 0.05)g. All five bottles was put in the mechanical shaker for 5mins, afterwards centrifuged for 15min. The centrifuged result was analyzed by the AAS to get the optimum dosage.

Effect of Contact Time Study

This study was carried out to vary time at different intervals (5, 20, 35, 50, 65)mins. To know at what particular time the adsorbent (MgO NP) adsorb the heavy metals in the water the

most hence, the optimum time. This was investigated thus, 0.05g of the adsorbent (Mg ONP) was accurately weighed into a polyethylene bottle, 100mL of a prepared 5ppm Cd^{2+} working solution was measured into 5 bottles with the time tag (5-65mins). All five (5) bottles were put into a mechanical shaker. At the said time intervals (5-65) mins all same were taken out of the shaker singly and then centrifuged for 15mins. The centrifuged samples were analyzed using the atomic absorption spectrophotometer to get the optimum contact time.

Effect of pH

pH was varied at different intervals (pH=2, 4, 6, 8, 10) to know at what pH did the heavy metals get adsorbed by adsorbent (Mg ONP) hence, the optimum pH. 100mL of the prepared 5ppm Cd^{2+} working solution was measured into 5 bottles, the pH of the 5 samples were adjusted to pH (2, 4, 6, 8,10) singly using a calibrated pH meter, 0.05g of the adsorbent was weighed into the samples. All five bottles was put into a mechanical shaker for 65mins. All samples were centrifuged for 15mins. All centrifuged samples were analyzed by the atomic absorption spectrophotometer to get the optimum pH.

Characterization of MgO Nanoparticles

MgO nanoparticles were characterized using FITR, XRD, SEM and UV-Vis spectrophotometry.

Fourier Transform Infrared Spectroscopy Analysis

FTIR is a technique for figuring out a material's surface chemistry. It can be used to determine which functional group(s) the sample's phytoconstituents will have. Infrared light is used in this technique to scan test materials and examine their chemical composition. The equipment determines which wavelength is absorbed after exposing the material to various wavelengths. Most frequently, organic compounds and occasionally inorganic molecules are both detected using FTIR. In a molecule, it also identifies the chemical bonds.

Scanning Electron Microscopy Studies

SEM produces complex, high-magnification images by using a focused electron beam to produce a variety of signals that can be utilized to learn more about the surface composition and topography.

X-Ray Diffraction

An X-ray beam is pointed at a sample to carry out the XRD, which is used to examine the structure of materials. It can reveal information about the dimensions of unit cells and is mostly used to determine the phase of crystalline materials. A crystalline structure is characterized by improved layer alignment, which is suggested by the sharp peak (Saied *et al.*, 2021).

Ultraviolet-Visible (UV-vis) Spectroscopy

UV-vis spectrophotometers calculate the wavelength-dependent absorbance or transmittance of light flowing through a material. UV-vis detectors are integrated into high performance liquid chromatography and ultra-high performance liquid chromatography to identify and measure the concentration of chemicals in liquid streams (Rocha *et al.,* 2018)

Adsorption Isotherm

Langmuir Model

According to the Langmuir isotherm model, monolayer adsorption occurs when a finite number of identical sites are used to adsorb the solute. The following equation can be used to represent the model of the nonlinear Langmuir isotherm:

$$q_e = q_{max} \left(\frac{K_L C_e}{1 + K_L C_e} \right)$$

q_e (mg/g) is the amount of solute adsorbed on the adsorbent surface at equilibrium
q_{max} (mg/g) is the maximum adsorption capacity
K_L (L/mg) is the Langmuir constant (Mohamed *et al.*, 2023)

Freundlich Model

According to the Freundlich isotherm model, the solute is simultaneously adsorbed with a large number of different sites on a variety of heterogeneous surfaces. Non-ideal adsorption can often be described using the Freundlich model. The hypothetical equation is:

$$q_e = K_F (C_e)^{1/n}$$

The Freundlich constant is Kf, while the empirical constant 1/n indicates the adsorption capacity of the solution. The isotherm is linear and the adsorption sites are uniform if n is equal to one (as in the Langmuir model); when n is less than one, the presence of more adsorbate in the absorbent raises the free energies of further adsorption; and if n is higher than one, the newly added adsorbates are bound with weak free energies (Mohamed *et al.*, 2023)

Temkin Model

The Temkin isotherm model is based on the supposition that as the adsorbent surface coverage rises, the adsorption heat of the solute falls linearly. Additionally, this isotherm makes the assumption that the adsorption up to the maximal binding energy follows the same distribution of binding energies. The Temkin isotherm can be explained using the following equation:

$$q_e = \frac{RT}{A_T} In A_T + \frac{RT}{A_T} Ln C_e$$

The universal gas constant is R (8.314 J/K.mol), whereas the temperature is T(k), the adsorption heat is represented by b, and the Temkin equilibrium binding constant is kT(L/mol) (Mohamed *et al.*, 2023)

Dubinin–Radushkevich Model

In order to explain the adsorption mechanism with the distribution of Gaussian energy onto heterogeneous and homogeneous surfaces, the Dubinin-Radushkevich (D-R) isotherm model is typically used. This physical adsorption system (multilayer adsorption) uses an adsorption model that is based on the pore-filling mechanism. The hypothetical equation is:

$$q_e = (q_{max}) \exp(-K_{ad} \varepsilon^2)$$
$$\varepsilon = RTIn\left(1 + \frac{1}{C_e}\right)$$

Dubinin–Radushkevich isotherm constant is k_{DR} (mol^2/KJ^2) and ε is the adsorption potential (Mohamed *et al.*, 2023).

RESULTS AND DISCUSSION
RESULT FOR THE CHARACTERIZATION OF MgO NPs
FTIR Result
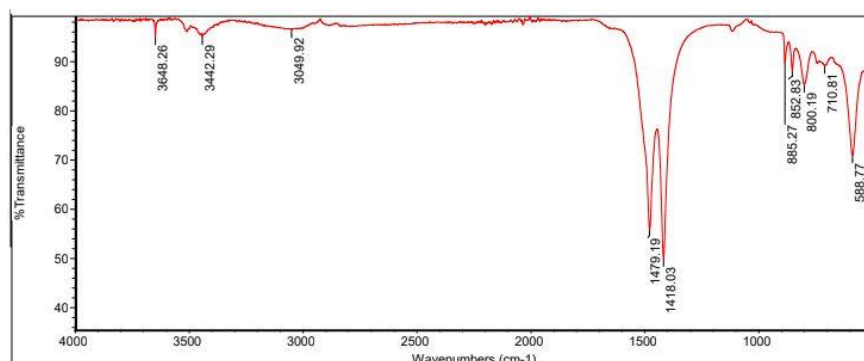
Figure 3.1: The FT-IR spectrum of bio-synthesized MgO NPs using Elephant grass.

The result of the FTIR analysis in Fig 3.1 showed that several intense absorption peaks appeared at 3648.26, 3442.29, 3049.92, 1479.19, 1418.03, 885.27, and 800.19 cm^{-1}. The peak observed at 3648.26 cm^{-1} signifies the –OH stretching band. The peak at 3442.29 cm^{-1} corresponds to hydrogen bonds arising from NH_2 and OH groups in protein molecules. The peak observed at 3049.92 corresponds to C-H stretch of alkene, the peak at 1479.19 is that C=C of arenes. The sharp peak at 1418.03cm^{-1} correspond to C-H bend of alkyl group. The peak at 885.27cm^{-1} correspond to C=C bending of alkene and 800.19cm^{-1} correspond to C-H bending 1, 2, 3-trisubstituted.

Figure 3.2: XRD of Magnesium Oxide Nanoparticles
The crystalline nature of biosynthesized MgO NPs was investigated using XRD analysis.
Debye Scherer's formula is used to find the particle size of synthesised MgO nanoparticles and the size was found to be 15.7nm. The results shows long tiny sharp peaks which talks about the well-ordered crystalline characteristics of the sample. The width of the peak is inversely proportional to the crystal size. A thinner peak corresponds to a bigger crystal. A broader peak means that there maybe a smaller crystal, defect in crystalline structure or that the sample might be amorphous in nature.
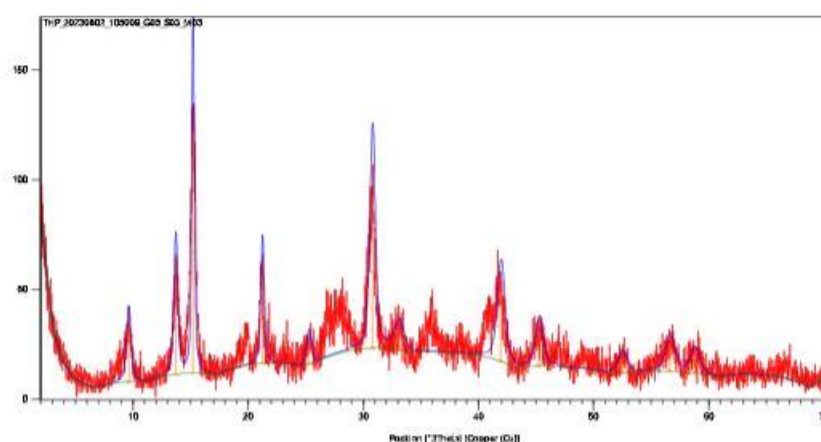
Figure 3.2 shows the XRD diffraction patterns of the prepared Magnesium Oxide nanoparticles.

Figure 3.3: The SEM-EDX analysis is well-thought-off as valuable procedure in the study of the topographical structure of biosynthesized MgO NPs, accumulation, and chemical compositions. The MgO NPs synthesized using elephant grass has homogenous surface with little roughness.
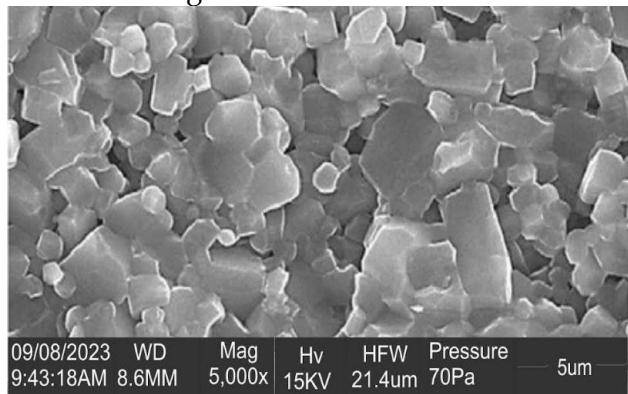
Figure 3.3: SEM Image of MgO NPs
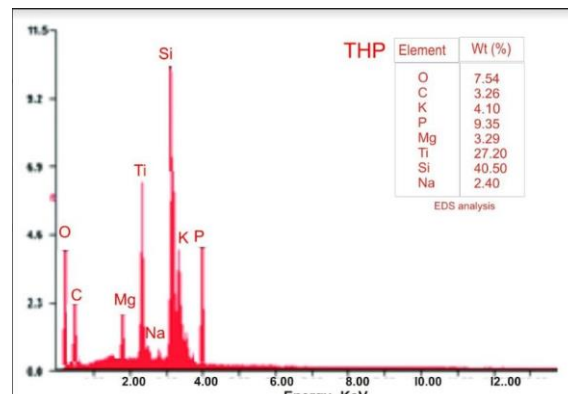
Figure 3.4: EDX of MgO NPs

The presence of Mg and O ions in the sample was confirmed by the EDX profile. The Data displayed the weight percentages of Mg and O were 3.29% and 7.54%, respectively (Figure 3.4). Additionally, the successful fabrication of MgONPs was confirmed by the presence of Mg peak at an energy of 0.2 to 1.8 KeV as shown in Figure 3.4. This result was also very close to that of Saied *et al.,* 2021.

Other elements such as C, Ti, Si, Na, K and P, on the other hand in the MgO NP sample were identified by EDX profiles with weight percentages of 3.26%, 27.20%, 40.50%, 2.40%, 4.10% and 9.35%, respectively. The presence of some impurities in the sample indicated by the presence of these additional peaks, which XRD analysis confirmed. The presence of additional peaks in the EDX profile were attributed by some investigators to the hydrolysis of enzymes, proteins, and other fungal metabolites that act as capping and stabilizing agents by X-ray (Jian *et al.,* 2019)

Adsorption Studies

Effect of Concentration on Adsorption of Cd^{2+} in Water

Table 3.2 shows the effect of different concentration (5, 10, 15, 20, 25) mg/L for cadmium ion in water. At constant volume (V=20ml) and constant adsorbent dosage = 0.01g, the adsorption efficiency was found to decrease on increasing the initial concentration of cadmium ion. It was noticed that when there were more metal ions in the beginning, the adsorption efficiency went down. At a low amount of cadmium ions to start with, all of them were stuck onto the adsorbent. This shows that when there are only a few cadmium ions, the adsorbent works really well. With a lot of metal in the beginning, the metal ions spread out more on the surface they stick to. The tiny holes in the absorbent material were blocked, making it hard for metal ions to go inside the holes. This means that absorption can only happen on the surface of the material. This means that if the places where the substance sticks were reduced, the substance would not stick as well (Mohamed *et al.,* 2023).

Table 3.2: Effect of Concentration on Adsorption of Cd^{2+} in Water.

Initial concentration C_o(mg/L)	Equilibrium concentration c_e(mg/L)	Amount absorbed (C_o-C_e) (mg/L)	Q_e(mg/g)	% Removal	C_e/Q_e (g/L)	Log C_e	Log Q_e
5	1.463	3.537	7.074	70.74	0.207	0.165	0.849
10	5.238	4.762	9.524	47.62	0.549	0.719	0.979
15	10.852	4.148	8.296	27.65	1.308	1.036	0.919
20	14.722	5.278	10.556	26.39	1.395	1.168	1.024
25	19.543	5.457	10.914	21.83	1.791	1.291	1.038

As can be seen from table 3:2, an increase in initial concentration of Cd^{2+} from 5 to 25mg/g caused the adsorption efficiency to decrease from 70.74 to 21.83%. Due to lack of active site and saturation of adsorption site, an increase in initial concentration led to reduced removal efficiency because absorbent dose was constant.
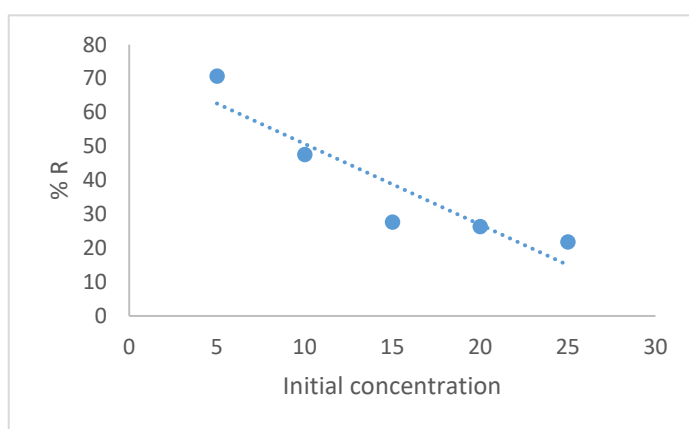
Figure 3.5: Graph of Percentage Removal against Initial Concentration

Effect of Adsorbent Dosage on Cd^{2+} Contaminant in Water
Table 3.3 shows the effect of different adsorbent dosage (0.01-0.0.5) g of cadmium ion in water. At constant volume (V=20ml) and constant initial concentration (5ppm), the adsorption efficiency was found to increase on increasing adsorbent dosage.
Increasing the dose of the sorbent leads to greater removal of metal ions due to the greater number of active sites available, the greater availability of the exchangeable sites or surface area at a higher dose of the adsorbent. The same pattern of adsorption of heavy metals were also observed by other researchers (Mohamed *et al.,* 2023).

Table 3.3: Effect of Adsorbent Dosage on Cd^{2+} Contaminant in Water

Adsorbent dosage (g)	Equilibrium concentration C_e(mg/L)	Amount absorbed (C_o-C_e) (mg/L)	% E
0.01	1.46	3.54	70.8
0.02	1.04	3.96	79.2
0.03	0.83	4.17	83.4
0.04	0.56	4.44	88.8
0.05	0.38	4.62	92.4

Table 3.2 shows that percentage removal increased with increasing adsorbent dosage. The highest removal was observed at adsorbent dosage of 0.05g.
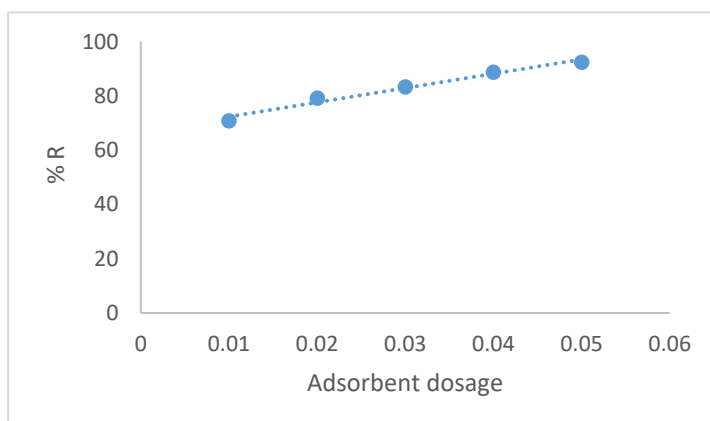
Figure 3.6 Graph of Percentage Removal against Adsorbent

Effect of Contact Time on Adsorption of Cd^{2+} in Water

Table 3.4 shows the effect of different contact time (5-65)mins on the adsorption of cadmium ion in water. At constant volume (V=20ml) and constant adsorbent dosage (0.05g) at constant initial concentration of 5ppm, the rate of adsorption was found to increase. Increasing the dose of the sorbent leads to greater removal of metal ions due to the greater number of active sites available, the greater availability of the exchangeable sites or surface area at a higher dose of the adsorbent. The same pattern of adsorption of heavy metals were also observed by other researchers (Mohamed *et al.*, 2023).

Table 3.4: Effect of Contact Time on Adsorption of Cd^{2+} in Water

Time (mins)	Equilibrium concentration c_e(mg/L)	Amount absorbed $(C_o\text{-}C_e)$ (mg/L)	% Removal
5	0.38	4.62	92.4
20	0.078	4.922	98.44
35	0.011	4.989	99.78
50	0.001	4.999	99.98
65	0.001	4.999	99.98
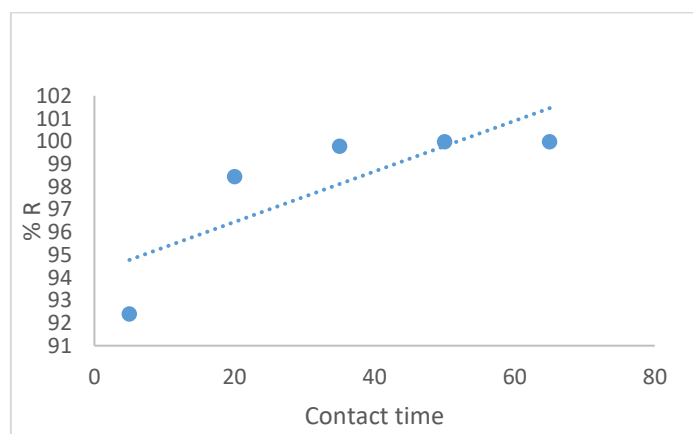
Figure 3.7 Graph of Percentage Removal against Contact Time

Effect of pH on Cd²⁺ Contaminant in Water

With reference to table 3.5, the effect of different pH (2, 4, 6, 8, 10) on the adsorption of cadmium ion in water at constant volume (V=20ml) and constant adsorbent dosage (0.05g) at constant initial concentration of 5ppm is shown. The rate of adsorption was found to increase. The reason why very little metal was removed at a low pH is because there was a competition between metal ions and protons for places to attach to. The places where the metal ions attach to on the nanoparticles are already occupied by protons. This explains why there was very little attachment of Cd^{2+} ions at a highly acidic pH. The results from the experiment showed that as the pH of the solution increased, the amount of material it could absorb also increased. The reason why metal ions adsorb more at higher pH levels could be because the hydrogen ions (H+) are also competing for the same adsorption spots, which makes it harder for the metal ions to adsorb. Other scientists have also seen similar patterns of heavy metals sticking to things more at higher pH levels (Mohamed *et al.*, 2023).

Table 3.5: Effect of P^H on Cd²⁺ Contaminant in Water

P^H	Equilibrium concentration c_e(mg/L)	Amount absorbed (C_o-C_e) (mg/L)	% Removal
2	2.325	2.675	53.5
4	1.98	3.02	60.4
6	1.091	3.909	78.18
8	0.89	4.11	82.2
10	0.73	4.265	85.3
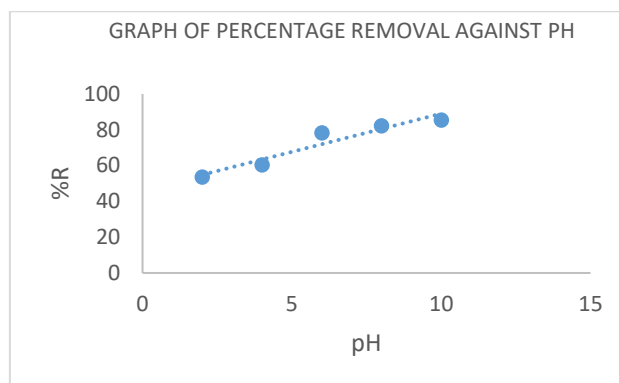
Figure 3.8 Graph of Percentage Removal against pH

Adsorption Isotherm

Adsorbent dosage at a constant concentration of 5 mg/L was used in the Adsorption Isotherm investigations to derive an approximation of the adsorption capacity of an adsorbent and the intensity of the heavy metal ions absorption.

Figure 3.9 shows Langmuir Adsorption Isotherm for Cadmium Ion and figure 3.10 shows Fruendlich Adsorption Isotherm for Cadmium Ion

LANGMUIR ADSORPTION ISOTHERM FOR CADMIUM ION

y = 10.908x - 1.0893
R^2 = 0.9657
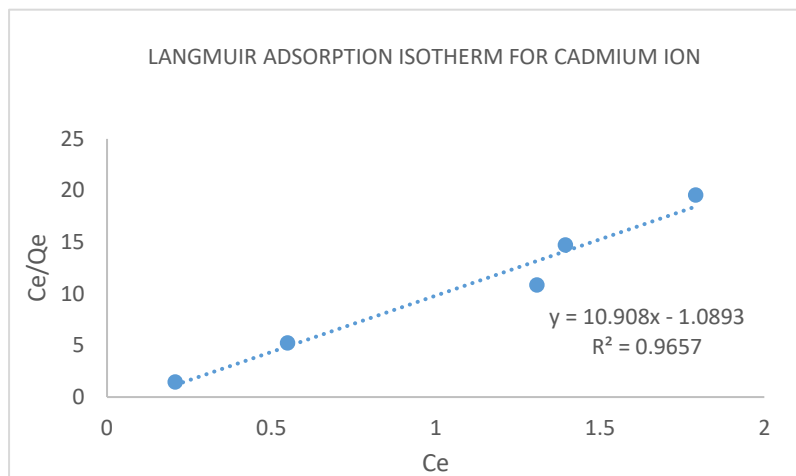
Figure 3.9 Langmuir Adsorption Isotherm for Cadmium Ion

y = 4.9105x - 3.8471
R^2 = 0.7272
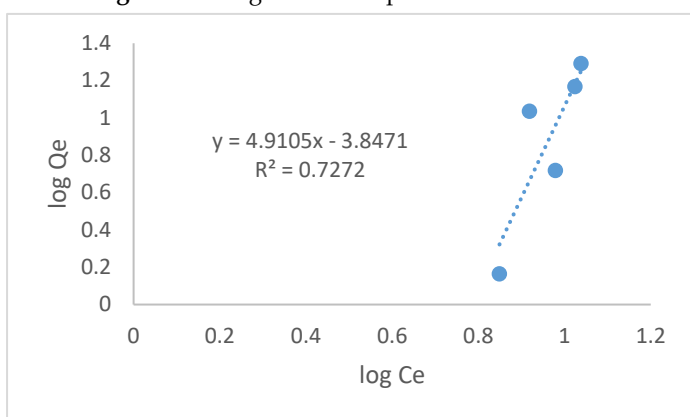
Figure 3.10 Fruendlich Adsorption Isotherm for Cadmium Ion

From table 3.2, the graph using the Freundlich equation displays the relationship between log Qe on the y-axis, and log Ce on the axis, where it is a straight line graph showing that that the isotherm is valid, whereas the graph using the Langmuir equation displays the relationship between Ce/Qe on the y-axis and Ce on the x-axis. In Langmuir , there is an increase in both axis, leading to the determination of a straight line graph which further accounts for the equilibrium between the adsorbate and adsorbent.

Conclusion

Magnesium oxide nanoparticles were synthesized using elephant grass extracts. Adsorption isotherm models indicated that Langmuir isotherm is the best model to describe the adsorption of Cd^{2+} on magnesium oxide nanoparticles prepared by elephant grass extracts. It was found that a removal of greater percent of Cd^{2+} could be accomplished through adsorption with 0.05g of magnesium oxide nanoparticles, an initial concentration of metal at 5ppm pH of 10 and at contact time of 65minutes

References

Esa, Y.A.M. and Sapawe, N., (2020). A short review on zinc metal nanoparticles synthesize by green chemistry via natural plant extracts. *Materials Today: Proceedings*, 31, pp.386-393.

Fatiqin, A., Amrulloh, H. and Simanjuntak, W., (2021). Green synthesis of MgO nanoparticles using Moringa oleifera leaf aqueous extract for antibacterial activity. *Bulletin of the Chemical Society of Ethiopia*, 35(1), pp.161-170.

Jian, W., Ma, Y., Wu, H., Zhu, X., Wang, J., et al., (2019). Fabrication of highly stable silver nanoparticles using polysaccharide-protein complexes from abalone viscera and antibacterial activity evaluation. *International journal of biological macromolecules*, 128, pp.839-847.

Khan, Y., Sadia, H., Ali Shah, S.Z., Khan, M.N., Shah, A.A., et al., (2022). Classification, synthetic, and characterization approaches to nanoparticles, and their applications in various fields of nanotechnology: A review. *Catalysts*, 12(11), p.1386.

Lee, Y.C., Moon, J.Y., Lee, Y.C. and Moon, J.Y., (2020). Introduction to nanotechnology and bionanotechnology. Introduction to bionanotechnology, pp.1-14.

Machado, S., Pacheco, J.G., Nouws, H.P.A., Albergaria, J.T. and Delerue-Matos, C., (2015). Characterization of green zero-valent iron nanoparticles produced with tree leaf extracts. *Science of the total environment*, 533, pp.76-81.

Mohamed, A., Atta, R.R., Kotp, A.A., Abo El-Ela, F.I., Abd El-Raheem, H., et al., (2023). Green synthesis and characterization of iron oxide nanoparticles for the removal of heavy metals (Cd2+ and Ni2+) from aqueous solutions with Antimicrobial Investigation. *Scientific Reports*, 13(1), p.7227.

Munjal, S., Singh, A. and Kumar, V., (2017). Synthesis and characterization of MgO nanoparticles by orange fruit waste through green method. *International Journal of Advanced Research in Computer Science*, 4(9), pp.36-42.

Nasrollahzadeh, M., Sajadi, S.M., Sajjadi, M. and Issaabadi, Z., (2019). An introduction to nanotechnology. In Interface science and technology (Vol. 28, pp. 1-27).

Rocha, F.S., Gomes, A.J., Lunardi, C.N., Kaliaguine, S. and Patience, G.S., (2018). Experimental methods in chemical engineering: Ultraviolet visible spectroscopy—UV-Vis. *The Canadian Journal of Chemical Engineering, 96(12), pp.2512-2517.*

Saied, E., Eid, A.M., Hassan, S.E.D., Salem, S.S., Radwan, A.A., et al., (2021). The catalytic activity of biosynthesized magnesium oxide nanoparticles (MgO-NPs) for inhibiting the growth of pathogenic microbes, tanning effluent treatment, and chromium ion removal. *Catalysts*, 11(7), p.821.

Saod, W.M., Oliver, I.W., Thompson, D.F., Holborn, S., Contini, A., et al., (2023). Magnesium oxide loaded mesoporous silica: Synthesis, characterisation and use in removing lead and cadmium from water supplies. *Environmental Nanotechnology, Monitoring & Management*, 20, p.100817.

Sathishkumar, M., Sneha, K., and Yun, Y.S. (2010). Immobilization of silver nanoparticles synthesized using Curcuma longa tuber powder and extract on cotton cloth for bactericidal activity. *Bioresource Technology*, 101(20), 7958-7965

Singh, T.A., Sharma, A., Tejwan, N., Ghosh, N., Das, J., et al., (2021). A state of the art review on the synthesis, antibacterial, antioxidant, antidiabetic and tissue regeneration activities of zinc oxide nanoparticles. *Advances in Colloid and Interface Science*, 295, p.102495.

Tinkov, A.A., Filippini, T., Ajsuvakova, O.P., Skalnaya, M.G., Aaseth, J., et al., (2018). Cadmium and atherosclerosis: A review of toxicological mechanisms and a meta-analysis of epidemiologic studies. *Environmental research*, 162, pp.240-260.

Zhou, Q., Yang, N., Li, Y., Ren, B., Ding, X., et al., (2020). Total concentrations and sources of heavy metal pollution in global river and lake water bodies from 1972 to 2017. *Global Ecology and Conservation*, 22, p.e00925.